JOURNAL OF MATERIALS SCIENCE 29 (1994) 3497–3504

Spiral growth mechanisms in partially melted bulk $YBa_2Cu_3O_{7-\delta}$

M. MARELLA, B.MOLINAS, B. BURTET FABRIS
TEMAV, Centro Ricerche Venezia, via delle industrie, 39, P.to Marghera, Venice, Italy

Large domains with platelets almost parallel to each other were obtained in bulk $YBa_2Cu_3O_{7-\delta}$ by a single-step partial melting procedure. The mechanisms of nucleation and growth of platelets are discussed. The nucleation of peritectic material from the liquid phase is favoured by heterogeneities in the melt. Experimental evidence of spiral growth of the nuclei in the [0 0 1] direction is given. Furthermore, structures of growth, which could also be an indication of spiral growth in the [0 1 0]/[1 0 0] directions, are shown. The final morphology of the domains can be explained on the basis of the periodic bond chain (PBC) theory if the growth rates of flat (F) faces of the platelets are dominated by kinetic coefficients which differ between them. The morphology of the as-grown (0 0 1) surface is explained in the framework of the PBC theory with the shape of the steps of macrospirals governed by the transition from roughness to smoothness of the liquid–solid interface. An account of large step heights is given by the model of giant screw dislocations caused by an impurity-induced lattice-constant gradient. Even higher step heights are correlated to the presence of obstacles and lack of liquid phase.

1. Introduction

An understanding of the growth mechanism of bulk partially melted $YBa_2Cu_3O_{7-\delta}$ can lead to improvements of the thermal treatment procedures with the aim of increasing the transport properties, particularly at high magnetic fields. The presence of dislocations in Type-II high-T_c superconductors is fundamental, because they can act as pinning centres of the magnetic field. In the case of *c*-axis oriented $YBa_2Cu_3O_{7-\delta}$ films, Mannhart *et al.* [1] reported the improvement of J_c with the increase of screw dislocation density in magnetic fields $\leqslant 0.1$ T, and attributed the improvement at higher fields to other defects correlated in growth to the screw dislocations, such as point defects or edge dislocations. For melt-processed $YBa_2Cu_3O_{7-\delta}$, the density of stacking faults at the interface of $YBa_2Cu_3O_{7-\delta}$ with entrapped Y_2BaCuO_5 particles also plays an important role.

The growth mechanism of $YBa_2Cu_3O_{7-\delta}$ single crystals, grown in a ZrO_2 crucible, was identified by Sun and Schmid [2] as a spiral growth for the basal {0 0 1} faces and as a probable two-dimensional nucleation for the lateral {0 1 0}/{1 0 0} faces. In the latter case the nucleation started at the crystal corners and edges, resulting in the observed hopper-like morphology. In a previous work [3], we found a similar morphology in the crystals freely grown into surface cavities of a partially melted sample. More recently [4], we observed macrospirals on the as-grown (0 0 1) surface. As far as we know, this was the first time that such a morphology had been reported on the external surface of large $YBa_2Cu_3O_{7-\delta}$ domains grown in partially melted bars. Jin *et al.* [5] found a spiral-like growth pattern on the (0 0 1) surface of $YBa_2Cu_3O_{7-\delta}$ sintered ribbons ($\simeq 6$ μm thick). They attributed the large step heights (10–100 nm) to the long heat treatment, and the driving force for the spiral-like growth to the recrystallization and coarsening of severely strained and finely pulverized $YBa_2Cu_3O_{7-\delta}$ phase.

A discussion of the mechanisms involved in the nucleation and growth of large $YBa_2Cu_3O_{7-\delta}$ platelets in partially melted samples is given below, as well as experimental support for the spiral growth in two perpendicular directions [0 0 1], [0 1 0]/[1 0 0].

2. Experimental procedure

Rods of partially melted $YBa_2Cu_3O_{7-\delta}$ with dimensions $3 \times 4 \times 45$ mm^3 were obtained with a single-step partial melting procedure without application of a temperature gradient on the sample. The specimens of precursor polycrystalline material were heated rapidly in flowing air to the semisolid region, where $YBa_2Cu_3O_{7-\delta}$ decomposes into Y_2BaCuO_5 and a Ba–Cu-rich liquid. They were held for some minutes, cooled quickly to some degrees above the peritectic solidification temperature and cooled extremely slowly (at 0.5 K h^{-1}) to ~ 6 °C below. Afterwards they were cooled to 900 °C (at 1 K h^{-1}) and extensively reoxygenated *in situ* while slowly cooled to room temperature, thus also ensuring stress relief. Details of the procedure were given previously [4].

Morphological observations were performed by optical microscopy and scanning electron microscopy (SEM), both instruments being connected to an image analyser; semiquantitative chemical analysis was

0022–2461

made by X-ray energy-dispersive analysis (EDXA); the lattice parameters of $YBa_2Cu_3O_{7-\delta}$ were determined by X-ray diffraction; the superconducting transition temperature was measured by a conventional four-probe technique on $1.0 \times 3.5 \times 12\ mm^3$ samples; hysteresis loops of the magnetization were measured on $6 \times 3 \times 1\ mm^3$ samples at liquid helium temperature up to 5 T, either with a squid magnetometer (H parallel to c-axis) or with a d.c. magnetometer (H perpendicular to c-axis), as shown elsewhere [6].

3. Results and discussion

The samples showed a domain microstructure, with stacks of parallel $YBa_2Cu_3O_{7-\delta}$ platelets, of typical dimensions of $3.5 \times 3.5\ mm^2$ cross-sectional area and with so far maximum dimensions of 12 mm length and 3 mm width [4]. Y_2BaCuO_5 and CuO particles are dispersed within the platelets. In Fig. 1 the fracture surface of part of a single domain is shown. The set of parallel lines correspond to sub-boundaries roughly parallel to the a–b planes which link the different platelets. The lattice parameters were: $a = 0.3832$ nm, $b = 0.3885$ nm, $c = 1.1677$ nm, with a slight shift towards a tetragonal structure. The critical temperature was 92 K (T_c onset) and the $T_c(R = 0)$ was 89.5 K. From the hysteresis loops the anisotropic critical current densities, J_c, were evaluated using the Bean model and their values at $H = 1$ T were: $J_{C_{H\text{parallel to c-axis}}} = 2 \times 10^5\ A\ cm^{-2}$ and $J_{C_{\text{perpendicular}}} = 9 \times 10^4\ A\ cm^{-2}$ [7].

An explanation for the development of a domain microstructure can be given as follows: in the first stage of thermal treatment the $YBa_2Cu_3O_{7-\delta}$ grains of small dimensions (typical diameter 20–30 μm) are decomposed into Y_2BaCuO_5 and a Ba–Cu-rich liquid. When the temperature is lowered to the peritectic one, the liquid has a composition in equilibrium with the Y_2BaCuO_5 and the $YBa_2Cu_3O_{7-\delta}$ phases, with no driving force for $YBa_2Cu_3O_{7-\delta}$ formation. On further cooling, as suggested by St John [8] and developed by Bateman *et al.* [9], it is probably easier to grow Y_2BaCuO_5 instead of nucleating $YBa_2Cu_3O_{7-\delta}$. On subsequent cooling the liquid composition follows the extended Y_2BaCuO_5 liquidus and at some stage a driving force for the crystallization of $YBa_2Cu_3O_{7-\delta}$ is generated. The liquid shifts towards a composition richer in Ba–Cu and the Y_2BaCuO_5, which is unstable, dissolves, bringing the liquid composition towards one poorer in Ba–Cu. However, the liquid becomes undercooled with respect to $YBa_2Cu_3O_{7-\delta}$, which can thus grow. The above mechanism, instead of being the nucleation of $YBa_2Cu_3O_{7-\delta}$ on Y_2BaCuO_5 followed by the thickening of $YBa_2Cu_3O_{7-\delta}$ by solid-state diffusion, as suggested by many authors, consists in the direct nucleation of $YBa_2Cu_3O_{7-\delta}$ from the liquid phase while Y_2BaCuO_5 dissolves in it. Heterogeneities in the melt act as preferred nucleation sites. Concentration gradients in the liquid, caused by the primary solid removing solute from the liquid, will also favour nucleation of the peritectic product away from the primary solid [8].

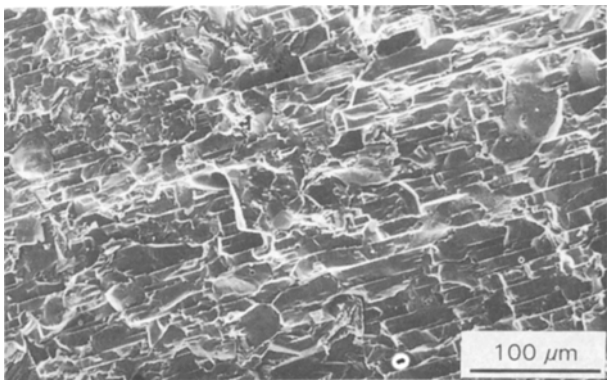

Figure 1 SEM fractography of a $YBa_2Cu_3O_{7-\delta}$ domain showing that the a–b planes of the platelets are almost parallel to each other.

Then the classical equation of the nucleation rate for homogeneous nucleation should be applicable

$$J = J_0 \exp[-16\pi \gamma_{sl} \Omega^2 / 3k^3 T^3 (\ln S)^2] \quad (1)$$

where J is the rate of nucleation, the number of nuclei formed per unit volume per unit time, J_0 is a pre-exponential factor, γ_{sl} is the interfacial energy per unit area of solid–liquid interface, Ω is the molecular volume, k is the Boltzmann constant, T the absolute temperature, and S the coefficient of supersaturation [10]. In this respect, a similarity with the nucleation (and subsequent growth) of single crystals from the melt is established.

After nucleation, the growth of domains can be explained, in our opinion, on the basis of the periodic bond chain (PBC) theory [11, 12] and a proposal of the possible mechanism will be given below. Here we briefly recall that the PBCs are uninterrupted sequences of periodically repeated strong bonds in crystallographic directions and that three categories of faces are distinguished: flat (F) containing two or more non-parallel PBCs in a layer of thickness d_{hkl}, stepped (S) containing only one, and kinked (K) containing none. The kinked faces do not require nucleation and are normally not present in the final morphology; the stepped faces grow by a one-dimensional nucleation, they are corrugated in a direction perpendicular to the PBC direction and sometimes appear so on a microscopic scale. The flat faces are slow growth faces, which grow by a two-dimensional nucleation or by a spiral growth mechanism, and are usually the only ones to determine the final habit of the crystal.

The PBC analysis was applied to $YBa_2Cu_3O_{7-\delta}$ single crystal by Sun *et al.* [13]. On the basis of the broken bond and electrostatic point charge models, the order of decreasing morphological importance for the tetragonal $YBa_2Cu_3O_6$ was

$$\{0\,0\,1\} \gg \{0\,1\,1\} > \{0\,1\,3\} > \{1\,1\,4\} \simeq \{1\,1\,2\}$$

while $\{0\,1\,0\}$ was an S form. The theoretical habit, determined by the first two forms, was predicted to be tabular to platy $\{0\,0\,1\}$, with $\{0\,1\,1\}$ as side faces.

In the case of $YBa_2Cu_3O_7$, $\{0\,1\,0\}$ becomes an F form, the habit is isometric with large $\{0\,0\,1\}$ and $\{0\,1\,1\}$ faces while the $\{0\,1\,0\}$ faces are small. The experimental $YBa_2Cu_3O_{7-\delta}$ habit was tabular, composed of $\{0\,0\,1\}$ and $\{0\,1\,0\}$, the first one being the

most prominent form. The presence of {0 1 0} faces instead of {0 1 1} was ascribed to external factors, which slowed the growth of {0 1 0}.

Turning now to our partially melted samples with large domains, Fig. 2a shows the as-grown surface, viewed laterally by SEM. In the micrograph two platelets with their *c*-axis oriented towards the platelet thickness are clearly seen. The sub-boundaries between platelets are marked SB. The platelet to the right, the last to grow during the solidification of the material, shows a macrospiral (top right) growing in the [0 0 1] direction. In previous work [4] we had already reported the evidence of spiral growth in this direction, but now we are able to show a structure of growth in a perpendicular direction on the same platelet (SG in Fig. 2a), which can also be an indication of spiral growth. The situation is better explained by the drawing derived by Hartman [12], Fig. 2b. In the case of Fig. 2a, the *a*- and *b*-axes may be interchanged. The flat face containing the non-parallel *a*- and *b*-PBCs is the top face of the macrospiral, the F face containing the *c*- and *b*-PBCs contains the region marked SG. It should be noted that this face is in its first stages of growth, as demonstrated by the reduced extension of the area around the spiral and by the stepped face connecting the two flat faces. The flat face containing the *a*- and *c*-PBCs, perpendicular to the former ones, has undergone a major process of growth, as demonstrated by the platelet extending downwards.

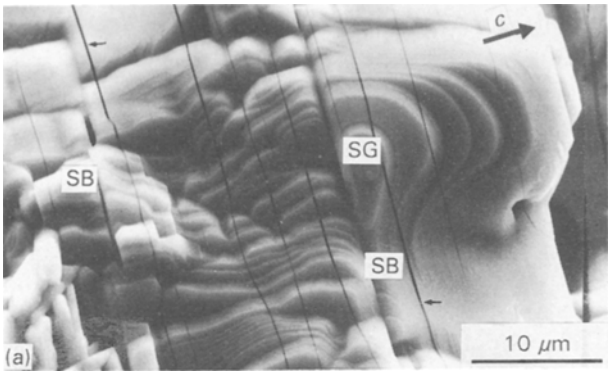

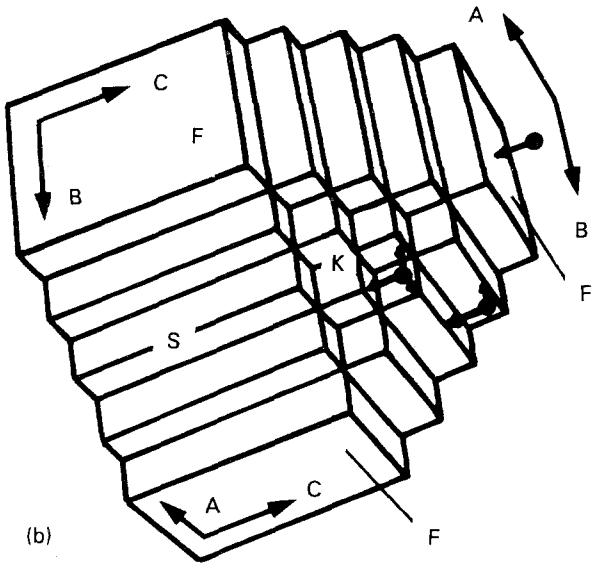

Figure 2 (a) Lateral view (SEM) of the as-grown surface of a partially melted sample. The sub-boundaries are marked SB. The region marked SG shows a spiral-like structure of growth in a direction perpendicular to the spiral growth along the *c*-axis. Two cracks are marked by arrows. (b) Hypothetical crystal with three PBC vectors: A// [1 0 0], B// [0 1 0], C// [0 0 1]. Flat (F), stepped (S) and kinked (K) faces are {1 0 0}, {1 1 0} and {1 1 1} faces (after Hartman [12]). The drawing closely reproduces the situation of top right platelet in (a).

Within each platelet several cracks, almost parallel to each other and perpendicular to the *c*-axis, are present; two of them are marked by arrows. Goyal *et al.* [14] demonstrated that in melt-processed $YBa_2Cu_3O_{7-\delta}$ the {0 0 1}, {1 0 0} and {0 1 0} planes are the preferred fracture planes and that the critical stress intensity factor for propagating a crack on the {0 0 1} basal plane is the lowest: $K_c^{001} < K_c^{100}$ or K_c^{010}. So cracks tend to form preferentially on {0 0 1} planes and {0 0 1} platelet boundaries, and are due to the highly anisotropic thermal expansion coefficients of $YBa_2Cu_3O_{7-\delta}$, particularly in mechanically constrained domains.

In Fig. 3 another example of two spirals growing in perpendicular directions is shown. Because little or no growth is expected for two-dimensional growth at low values of supersaturation and as the partially melted samples grow along the [0 0 1] direction by spiral growth as the single crystal do, the final experimental morphology of the domains of partially melted samples, with platelets grown much more along the [0 1 0]/[1 0 0] directions, cannot be explained if we do not assume a spiral growth also along these directions. So the growth mechanism of flat {0 1 0}/{1 0 0} faces differs from that of single crystals. The as-grown (0 1 0)/(1 0 0) surface of a different domain is shown in Fig. 4: two step trains are visible, the centre of each being localized at the two extremities.

The origin of spiral growth could be dislocations crossing the surface with Burgers vectors making different angles with it. As summarized by Chernov [15], a spiral can grow around the outcrop of dislocations crossing the surface and having a non-zero Burgers vector component normal to this surface, i.e. $\boldsymbol{b}_N \neq 0$. The solution has to be supersaturated on the surface.

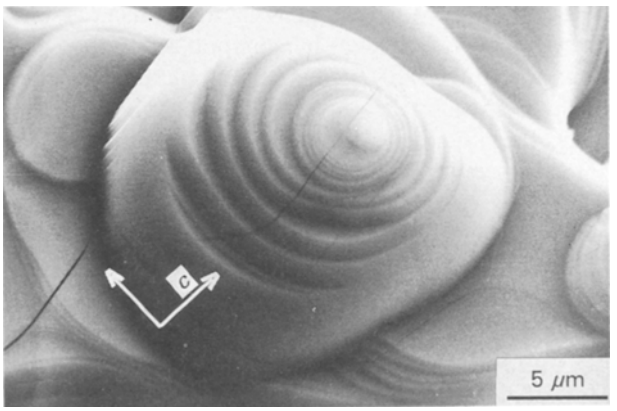

Figure 3 Scanning electron micrograph of the early stages of growth of a platelet on the as-grown (0 0 1) surface. The spiral growth is in two perpendicular directions, as shown by the arrows.

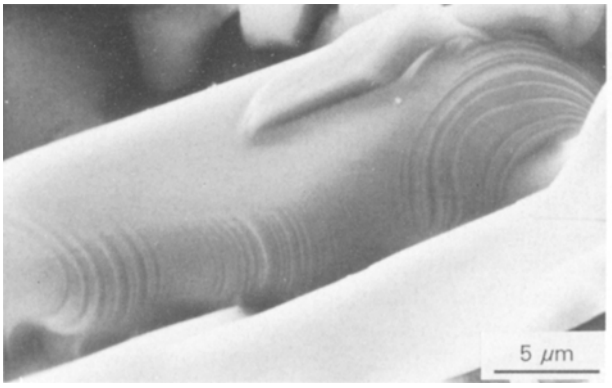

Figure 4 Scanning electron micrograph of the as-grown (0 1 0)/(1 0 0) surface of a different domain; step trains are shown.

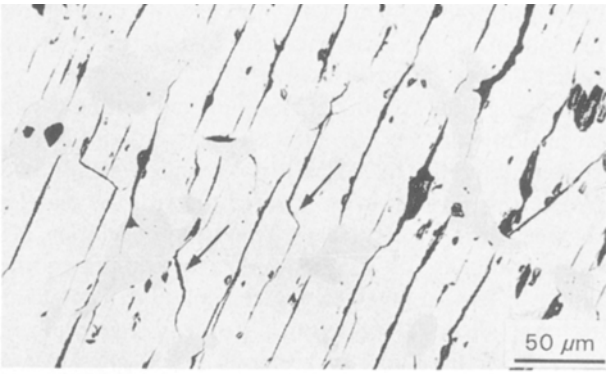

Figure 6 Optical micrograph of a $YBa_2Cu_3O_{7-\delta}$ domain. The situation reported in Fig. 5 at $t = t_3$ is marked by arrows.

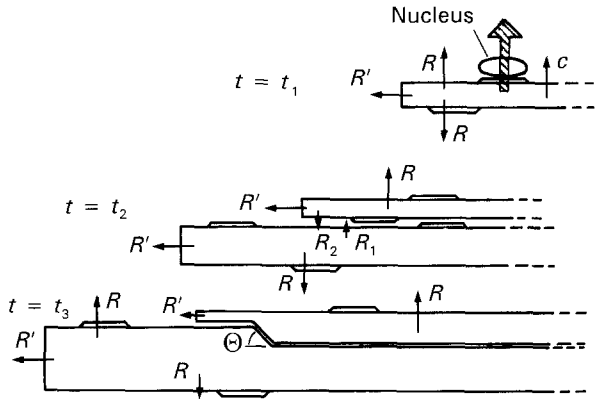

Figure 5 Growth scheme of two platelets in a $YBa_2Cu_3O_{7-\delta}$ domain (extension to n platelets in the domain is straightforward). Growth spirals and growth rates at different positions are also shown.

Occasionally, the growth layers (i.e. the steps) can also be generated by edge dislocations, or more exactly dislocations with $\boldsymbol{b}_N = 0$. For the case of edge dislocations and under large supersaturation it has been observed that the spiral growth steps are replaced by concentric ones.

On the basis of the results shown in the Figs 2a, 3 and 4, after nucleation the following growth mechanism of a domain can be envisaged. With reference to Fig. 5, at the time $t = t_1$, a pre-existing platelet, which is growing by a spiral growth mechanism with a growth rate $R' \gg R$, gives information about the c-axis direction to the nucleus of a second platelet. The new nucleus grows by the same mechanism and at the time $t = t_2$ the situation is as reported in the figure, with R_1 somehow dependent on R_2 and both lower than R. This process can repeat itself for the number, n, of platelets inside the domain. At the time $t = t_3$, the difference in the growth rates R_2 and R can lead to the formation of a grain boundary forming an angle θ, as shown in Fig. 6. This defect is commonly found in our samples and it seems to be a typical defect which can also be observed in many literature micrographs. Because $R' \gg R > R_1 \simeq R_2$, the situation reported at the time $t = t_3$ does not affect all the platelets and the domains can grow with platelets almost of the same thickness and parallel to each other up to the impingement of different domains, where the platelets meet with high-angle boundaries.

Jackson [16] calculated the change in free energy, ΔG, on adding extra atoms to a fraction, χ, of the N possible sites on an initially plane interface at the equilibrium temperature, T_0

$$\Delta G/NkT_0 = \alpha\chi(1-\chi) + \chi\ln\chi + (1-\chi)\ln(1-\chi) \quad (2)$$

where

$$\alpha = \xi L/kT_0 \quad (3)$$

where ξ is related to the crystallographic anisotropy, L is the latent heat of melting, k is the Boltzmann constant.

If a plot of Equation 2 is made for $\alpha > 2$, the lowest free-energy configuration changes from half the available sites filled (rough interface) to a few extra sites filled and a few atoms missing from the layer (smooth interface). So α is a measure of the roughness of the interface and from Equation 3, the lower the temperature of growth the smoother is the interface. Also the supersaturation (or the undercooling) plays an important role, and faces with α just a little greater than 2, which are smooth at the equilibrium temperature, may become rough when the supersaturation increases [17]. In the case of bulk partially melted $YBa_2Cu_3O_{7-\delta}$, when the interface is rough, the steps of the spirals on the (0 0 1) surface can grow independently of the crystallographic directions and their shape is near circular. When the interface becomes rougher and rougher the steps are forced to follow the crystallographic directions, the next-strongest ⟨1 1 0⟩ PBC directions where the kink density is lower and the strongest ⟨0 1 0⟩/⟨1 0 0⟩ PBC directions where the kink density is even lower. So, on decreasing the roughness, there is a transition from circular to octagonal to square (or rectangular) in the morphology of the spirals. In a previous work [4], scanning electron micrographs of octagonal and rectangular macrospirals were shown. Another example of well-defined macrospirals is shown in Fig. 7. In Fig. 8 it is seen that the above sequence is sometimes more complicated: (a) on the bottom the shape is octagonal,

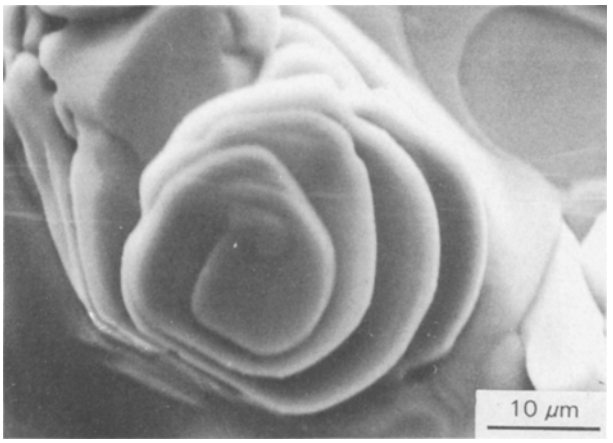

Figure 7 Scanning electron micrograph of a macrospiral growing on the (0 0 1) surface. Regularity in the spacing of the macrosteps is shown.

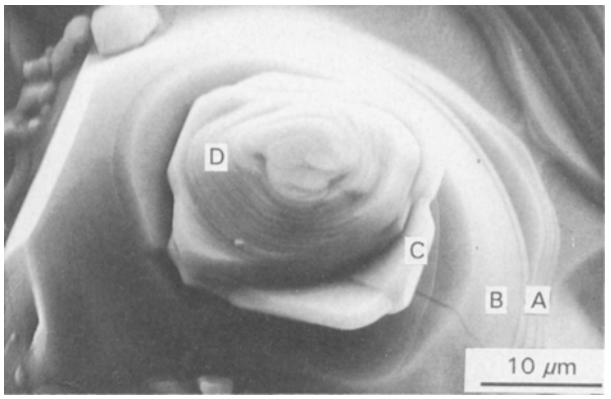

Figure 8 Scanning electron micrograph of a complex shaped macrospiral. Inversions of trend in the usual sequence circular–octagonal–square shape are shown from the bottom to the top: A = octagonal, B = near circular, C = octagonal almost square, D = near circular shapes.

(b) subsequently it becomes near circular, (c) then octagonal almost square, and (d) again circular. If, as it seems probable, the most elevated steps grow at a later stage when the growth temperature is lower, from (a) to (b) or from (c) to (d) there are inversions of trend. This fact could be due to the presence of thermal fluctuations in the melt during growth, but we must also take into consideration the effect of supersaturation, as explained above. So, being in the region of a transition from rough to smooth interface, the most probable reason is a combined effect of temperature and supersaturation which readily plays for one or the other: as the temperature decreases the interface becomes smooth, but also the supersaturation increases, which cause it to become rougher again. Other interesting features concern the role of inclusions during the growth of the macrospirals. In Fig. 9 we show the influence of the inclusions on the geometry of the steps of macrospirals. A macrospiral was growing with octagonal shape. Two particles of Y_2BaCuO_5, whose composition was revealed by

Figure 9 Scanning electron micrograph of an octagonal-shaped macrospiral distorted during the growth by the presence of two Y_2BaCuO_5 particles.

EDXA, were located on the top of the spiral during growth. This type of distortion resulted in a distortion of the octagonal shape. Furthermore, the upper surface was affected by the particles: the material grew following the shape and size of the inclusions and not the PBCs. This can explain the lack of regularity in the spacing of certain spirals observed in the present and in the previous work [4].

The presence of obstacles can also participate in the generation of spirals with coarser steps whenever the growth of the steps located in the lower position of the spirals is interrupted or the growth rate across the *a–b* plane is reduced. Also insufficient liquid phase can lead to an accumulation of steps in the external limits of a given region where the spiral is growing. These cooperative phenomena can thus give rise to "tall" steps on the as-grown (0 0 1) surface (see Figs 7 and 8). It should also be pointed out that the steps are only apparently coarse, because a finer submicronic structure can be seen, for example, in Fig. 10. The characteristics of these spirals, together with other types reported in the literature, are summarized in Table I.

Up to now, a possible explanation of the mechanisms of growth of a single domain and of the

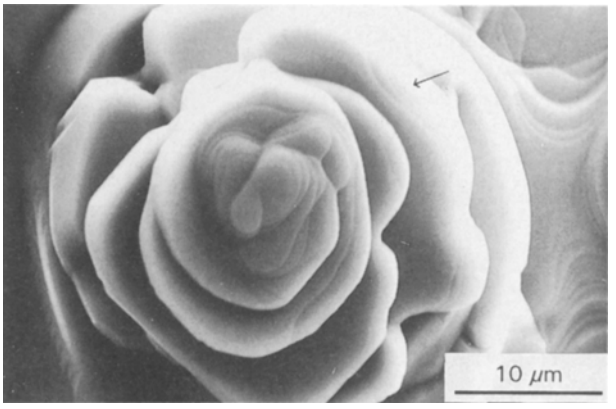

Figure 10 Scanning electron micrograph of a macrospiral with seemingly coarse growth steps. Finer structures in the submicrometre size range are marked by an arrow.

TABLE I Spiral characteristics in thin, thick films, single crystals and partially melted bulk $YBa_2Cu_3O_{7-\delta}$

Spiral type	Kind of material	Type of microscopy[a]	Diameter (μm)	Step height (μm)	Spacing between steps (μm)	Total height	Reference
Microspiral	Thin film	STM	0.2–0.7	–	0.03–0.06	–	[18]
Spiral growth pattern	Thin film	STM	–	$(0.6–2.4)\times10^{-3}$	–	–	[20]
Spiral-like growth	Thick film	SEM	$\simeq 5$	0.01–0.1	–	–	[5]
Microspiral	Single crystal	STM	$\simeq 1.5$	1.16×10^{-3}	–	–	[21]
Macrospiral (normal growth)	Single crystal	Optical	60	Tenths of μm	8	μm	[19]
Macrospiral (conventional growth)	Single crystal	Optical DIC-Nomarski (after decoration)	50–125	Close to the limits of detection	1–10	–	[19]
Macrospiral (tall steps)	Bulk	SEM	20–40	1–3 (substeps < 1 μm)	3–5	15–30 μm	[4] and present work

[a]STM, Scanning tunnelling microscopy; DIC, Differential interference contrast.

morphology of the external (0 0 1) surface of the domain has been given. On the other hand, for the surfaces between the platelets, Fig. 11 shows the sub-boundary (0 0 1) between two of them as revealed by fracturing a single domain: step trains are readily observable and the step heights are in the submicrometre size range. These step trains are not markings left by a crack after its propagation but are growth steps. This fractographic method enables us to study the structure of the sub-boundaries.

In our opinion, the {0 0 1} surfaces of inner platelets behave quite similarly to those of single crystals during their growth. Therefore, those step trains may be related to the spiral growth mechanism acting between platelets, as shown in Fig. 5. On the contrary, the outermost surface of the platelets, which is also the surface of the specimen, is a special surface, in the sense that it is free to grow and is not constrained between platelets "welded" together. Also, liquid phases with comparatively larger amounts of impurities can be segregated on that surface as well as on the boundaries between different domains.

It still remains to be explained why the step heights either of the macrospirals on the as-grown (0 0 1) surface or on the {0 0 1} surfaces between platelets, are in the submicrometre size range, while lower values are expected in the case of a pure screw dislocation growth mechanism. A possible explanation comes from the model of Kuhlmann-Wilsdorf *et al.* [22], which accounts for growth steps of very large step heights, up to hundreds of nanometres, associated with a single giant screw dislocation in platelet crystals. Basically the model considers that a platelet in the early stages of growth must exhibit some lattice-parameter gradients due to changing impurity concentrations, which increase from the platelet centre (supposed pure) towards its periphery. Near the rim the hoop stresses will be compressive if the lattice constant increases towards the periphery, as for $YBa_2Cu_3O_{7-\delta}$ (see later). On the assumption of an initially roughly circular platelet, the hoop stresses can lead to cracking along the radial plane by a slip process or through brittle fracture. After cracking, the increasing lattice constants will lead to overlap and the tip of the crack will geometrically contain a giant screw dislocation, or better a superimposed giant screw dislocation and a disclination. The Burgers vector will be the thickness of the platelet when it first cracked or be simply related to it. Afterwards the crystal continues to grow by the propagation of the growth ledge of the overlapping crystal parts. Also, the slight twist-misfit between the two overlapping parts will automatically generate a twist boundary of screw dislocations parallel to the basal plane. It is thought that this last observation lends additional support to spiral growth in two perpendicular directions, as already suggested by Figs 2, 3 and 4. In fact the presence of such a network of screw dislocations located across the a–b plane may generate the dislocation outcrops around which the spiral growth takes place.

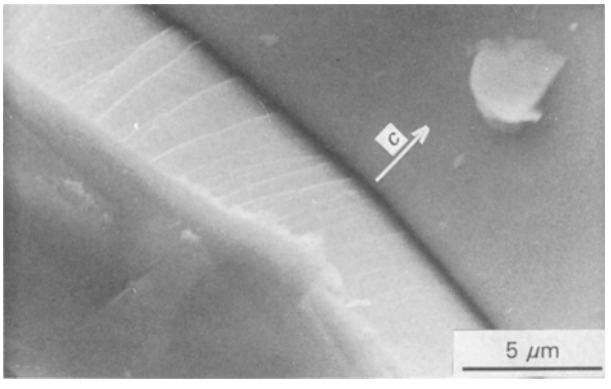

Figure 11 SEM fractography of a $YBa_2Cu_3O_{7-\delta}$ domain, showing growth pattern between two platelets. The step height is considerably lower than those of macrospirals on the as-grown (0 0 1) surface.

According to theory, the giant screw dislocations will form preferentially in crystals with large F values in the critical stage of crystal growth, where F is the platelet diameter-to-thickness ratio. The smallest F value that permits the formation of giant screw dislocation via glide is

$$ {}_sF_{crit} = {}_s(D/h)_{crit} \simeq 3/\Delta p \simeq a_0/\Delta a \qquad (4) $$

where D is the platelet diameter (supposed cylindrical), h is the platelet thickness, Δp the impurity concentration difference between the platelet periphery and its centre, a_0 is the lattice constant at the crystal centre, and Δa is the lattice constant difference.

From Equation 4 crystals with F ratios of the order of 100 might exhibit giant screw dislocations at impurity concentrations of about 1%, but not 0.1%, while crystals with still larger F values would require only quite small impurity levels for the generation of giant screw dislocations. Because the partial melting procedure was run using alumina supports, we measured the atomic ratio Y:Ba:Cu:Al of the platelets at several points by EDXA. The mean value was 1.17:2.02:2.79:0.02, corresponding to an aluminium impurity content of 0.7% with respect to copper. From the literature it is known that aluminium substitutes for copper in the Cu(1) site [23]. From Equation 4 the F value should be about 400 and, if the thickness of the steps, as shown in Figs 10 and 3, is about 0.1 μm, the smallest critical diameter would be 40 μm. Because the value of aluminium content is a mean of measurements mostly taken on inner platelets, an increase of aluminium on the surface, for the above reasons, is reasonable and would decrease the F value and thus the critical diameter below 40 μm.

We can also try to compare the F value obtained through impurity measurements with that of lattice parameter measurements. Several authors [23, 24] have demonstrated that $YBa_2Cu_{3-x}Al_xO_{7-\delta}$ tolerates a relatively high concentration of aluminium on the Cu–O chains, up to $x = 0.12$, though keeping a relatively high transition temperature (78 K). When aluminium substitutes to copper in the Cu(1) site, an octahedral oxygen coordination is preferred and this contributes to the increase cross-linking of the Cu–O chains. The effect is a shift of the structure towards a tetragonal one, as also reported above. This requires an increase in the a-lattice parameter, which, in our case, shifts from 0.3817 nm to 0.3832 nm, while b- and c-axes remain substantially unaffected. Taking into consideration only the difference in a-lattice parameters, the application of Equation 4 would give an ${}_sF_{crit}$ value of about 200 and a critical diameter of about 20 μm, with the usual assumption of a thickness of 0.1 μm. This result is in fairly good agreement with the value of about 400 obtained previously. However, it should be pointed out that these considerations refer to the final orthorhombic oxygenated structure obtained by our single-step partial melting procedure, while a demonstration of the effect of aluminium on the lattice parameter should be given on the tetragonal phase, the equilibrium phase at the temperature of growth. However, this would require the interruption of the thermal procedure, followed by quenching of the samples. Probably this stage could not be tolerated by the specimens in view of their full density. Also the surface morphology would be badly altered as a consequence of extensive cracking.

The Khulmann-Wilsdorf model can thus explain step heights with large Burgers vector, because this is related to the platelet thickness at the time of the first crack.

4. Conclusions

The microstructure of large $YBa_2Cu_3O_{7-\delta}$ domains with platelets almost parallel to each other can be explained for partially melted samples as follows.

1. $YBa_2Cu_3O_{7-\delta}$ nucleates directly from the melt and this process is favoured by heterogeneities and concentration gradients in the liquid.
2. $YBa_2Cu_3O_{7-\delta}$ nuclei grow by a spiral growth mechanism along the [0 0 1] direction, each nucleus receiving information about the c-axis orientation by an already growing platelet. The presence of growth structures in the perpendicular directions [0 1 0]/[1 0 0] may suggest a similar spiral growth mechanism. The final morphology can then be derived if we assume growth rates with quite different kinetic coefficients in the two directions.

The morphology of the as-grown (0 0 1) surface clarifies the former mechanism of growth because it shows the early stages of growth of a single platelet. The macrospiral shapes can be explained on the basis of PBC theory with the transition from a rough to a smooth interface playing a fundamental role. However, the step heights in the submicrometre size range can be accounted for only by the Khulmann-Wilsdorf giant screw dislocations mechanism, caused by impurity-induced lattice-constant gradient.

Finally, an explanation of "tall" steps associated to the presence of obstacles and to the lack of liquid phase is given.

Acknowledgement

The authors thank R. Guerriero and L. Meregalli for supporting the work, and A. S. Siri and C. Ferdeghini, Department of Physics, University of Genoa, for magnetic measurements.

References

1. J. MANNHART, D. ANSELMETTI, J. C. BEDNORZ, CH. GERBER, K. A. MÜLLER and D. G. SCHLOM, *Supercond. Sci. Technol.* **5** (1992) S125.
2. B. N. SUN and H. SCHMID, *J. Crystal Growth* **100** (1990) 297.
3. M. MARELLA, I. TANGERINI, B. BURTET FABRIS, G. DINELLI and S. VICARI, *J. Mater. Sci. Lett.* **11** (1992) 1367.
4. M. MARELLA, G. DINELLI, B. BURTET FABRIS and B. MOLINAS, *J. Alloys Comp.* **189** (1992) L23.
5. S. JIN, G. W. KAMMLOTT, S. NAKAHARA, T. H. TIEFEL and J. E. GRAEBNER, *Science* **253** (1991) 427.
6. M. R. CIMBERLE, C. FERDEGHINI and A. S. SIRI, *Cryogenics* **29** (1989) 69.
7. M. MARELLA, I. TANGERINI, B. BURTET FABRIS, G. DINELLI, S. VICARI, V. CALZONA, M. R. CIMBERLE, C. FERDEGHINI, M. PUTTI and A. S. SIRI, in Extended Abstracts of the 5th National Conference on High Transition Temperature Superconductivity SATT5, Capri, May 1992, edited by A. Di Chiara and M. Russo (Naples) p. 168.
8. D. H. St JOHN, *Acta Metall. Mater.* **38** (1990) 631.
9. C. A. BATEMAN, L. ZHANG, H. M. CHAN and M. P. HARMER, *J. Am. Ceram. Soc.* **75** (1992) 1281.
10. K. SANGWAL, in "Etching of Crystals", edited by S. Amelinckx and J. Nihoul (North-Holland, Amsterdam, 1987) p. 47.

11. P. HARTMAN and W. G. PERDOK, *Acta Crystallogr.* **8** (1955) 49.
12. P. HARTMAN, in "Crystal Growth–an Introduction", edited by P. Hartman (North Holland, Amsterdam, 1973) p. 367.
13. B. N. SUN, P. HARTMAN, C. F. WOENSDREGT and H. SCHMID, *J. Crystal Growth* **100** (1990) 605.
14. A. GOYAL, P. D. FUNKENBUSCH, D. M. KROEGER and S. J. BURNS, *J. Appl. Phys.* **71** (1992) 2363.
15. A. A. CHERNOV, *Z. Phys. Chem.* **269** (1988) 941.
16. K. A. JACKSON, in "Liquid Metals and Solidification" (American Society for Metals, Cleveland, OH, 1958) p. 174.
17. K. SANGWAL, in "Etching of Crystals", edited by S. Amelinckx and J. Nihoul (North-Holland, Amsterdam, 1987) p. 59.
18. H. P. LANG, H. HAEFE, G. LEEMAN and H. J. GÜNTHERODT, *Phys. C* **194** (1992) 81.
19. B. N. SUN, K. N. R. TAYLOR, B. HUNTER, D. N. MATHEWS, S. ASHBY and K. SEALEY, *J. Crystal Growth* **108** (1991) 473.
20. M. HAWLEY. I. D. RAISTRICK, J. G. BEERY and R. J. HOULTON, *Science* **251** (1991) 1587.
21. A. V. NARLIKAR, P. K. DUTTA, S. B. SAMANTA, O. N. SRIVASTAVA, P. RAMASAMY, S. C. SABARWAL, M. K. GUPTA and B. D. PADALIA, *J. Crystal Growth* **116** (1992) 37.
22. D. KUHLMANN-WILSDORF, D. PANDEY and P. KRISHNA, *Philos. Mag. A* **00-4** (1980) 527.
23. T. SIEGRIST, L. F. SCHNEEMEYER, J. V. WASZCZAK, N. P. SINGH, R. L. OPILA, B. BATLOGG, L. W. RUPP and D. W. MURPHY, *Phys. Rev. B* **36** (1987) 8365.
24. Y. XU, R. L. SABATINI, A. R. MOODENBAUGH, Y. ZHU, S.-G. SHYU, M. SUENAGA, K. W. DENNIS and R. W. McCALLUM, *Phys. C* **169** (1990) 205.

Received 18 March
and accepted 30 November 1993